BIOCHEMISTRY
including biophysical chemistry & molecular biology

ARTICLE

pubs.acs.org/biochemistry

Combined Genetic and Metabolic Manipulation of Lipids in *Rhodobacter sphaeroides* Reveals Non-Phospholipid Substitutions in Fully Active Cytochrome *c* Oxidase

Xi Zhang,[†,‡] Carrie Hiser,[†] Banita Tamot,[†] Christoph Benning,[†] Gavin E. Reid,[†,‡] and Shelagh M. Ferguson-Miller*[,†]

[†]Department of Biochemistry and Molecular Biology and [‡]Department of Chemistry, Michigan State University, East Lansing, Michigan 48824, United States

Supporting Information

ABSTRACT: A specific requirement for lipids, particularly cardiolipin (CL), in cytochrome *c* oxidase (C*c*O) has been reported in many previous studies using mainly in vitro lipid removal approaches in mammalian systems. Our accompanying paper shows that C*c*O produced in markedly CL-depleted *Rhodobacter sphaeroides* displays wild-type properties in all respects, likely allowed by quantitative substitution with other negatively charged lipids. To further examine the structural basis for the lipid requirements of *R. sphaeroides* C*c*O and the extent of interchangeability between lipids, we employed a metabolic approach to enhance the alteration of the lipid profiles of the C*c*O-expressing strains of *R. sphaeroides* in vivo using a phosphate-limiting growth medium in addition to the CL-deficient mutation. Strikingly, the purified C*c*O produced under these conditions still maintained wild-type function and characteristics, in spite of even greater depletion of cardiolipin compared to that of the CL-deficient mutant alone (undetectable by MS) and drastically altered profiles of all the phospholipids and non-phospholipids. The lipids in the membrane and in the purified C*c*O were identified and quantified by ESI and MALDI mass spectrometry and tandem mass spectrometry. Comparison between the molecular structures of those lipids that showed major changes provides new insight into the structural rationale for the flexible lipid requirements of C*c*O from *R. sphaeroides* and reveals a more comprehensive interchangeability network between different phospholipids and non-phospholipids.

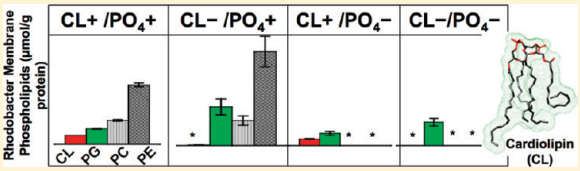

Lipid biosynthesis in bacteria is highly sensitive and adaptable to the growth medium.[1] In addition to modification by genetic mutations as described in the companion paper (DOI 10.1021/bi101702c), the lipid profile of bacteria can be modulated through metabolic approaches such as using low-phosphate growth medium.[1−4]Because limited phosphate in the growth medium affects all types of phosphate-containing lipids, this approach can be used as another tool to evaluate the functional significance of phospholipids and non-phospholipids in vivo, with respect to bacterial growth and the properties of well-characterized membrane proteins. Previous studies of both *Rhodobacter sphaeroides*[1] and *Sinorhizobium melitoti*[3,4] found that these bacteria are viable at phosphate concentrations as low as 0.1 mM (compared to the normal 20 mM[1]), but phosphate-limiting media significantly change the membrane lipid profile. The amounts of phospholipids are found to be significantly reduced, and novel types of phosphate-free lipids are produced in high abundance.[1]

Previous lipid biochemistry studies found that when grown in media containing abundant phosphate,[5,6] the membranes of wild-type *R. sphaeroides* strain 2.4.1 contain phosphatidylethanolamine (PE), phosphatidylcholine (PC), phosphatidylglycerol (PG), and cardiolipin (CL), and non-phospholipids such as sulfoquinovosyldiacylglyceride (SQDG) and ornithine lipids (OL), but phospholipids are the predominant components. Under phosphate-limiting growth conditions, the novel non-phosphate-containing glycolipids glucosylgalactosyldiacylglyceride (GGDG) and diacylglyceryl-*N*,*N*,*N*-trimethylhomoserine (DGTS) were produced, and the level of production of SQDG and OL was increased.[1] DGTS was proposed to functionally compensate for PC, SQDG for PG, and OL for PE, on the basis of the similarity of the charge state in the headgroup.[1,2,7] DGTS was also the predominant type of lipid in *S. melitoti* under phosphate-limiting growth.[3]

Mutations in genes involved in lipid synthesis can cause a specific deficiency in a particular type of lipid, such as PC, CL, or SQDG, but the amount of some other types of lipids was often seen to increase as well, interpreted as a compensatory mechanism for fulfilling the required biological functions.[5] Cardiolipin deficiency, which is often created by mutating the cardiolipin synthase,[8,9] produced an increased level of PG lipids.[9] Therefore, it is proposed that the high degree of structural resemblance of PG and CL makes PG the essential lipid that can functionally replace CL. On the other hand, SQDG and PG lipids appear to be interchangeable in *R. sphaeroides* because both have negative charge in the headgroup, and the depletion of both SQDG and PG is

Received: October 21, 2010
Revised: April 7, 2011
Published: April 08, 2011

lethal.[2] An effect of PE depletion on some membrane proteins can be restored by monoglucosyldiacyl-glycerol because of the similarity in the molecular shape.[10]

One question raised from a comparison of these previous findings is whether such types of functional compatibility are determined more by the phosphatidylglyceride backbone structure, by the negative or positive charge state, by the headgroup functional groups, or by the molecular shape. Because phosphate-limited growth can decrease the level of production of the entire set of phospholipids and increase the relative amount of polar non-phospholipids, its combination with the genetically produced specific lipid deficiency should be able to provide deeper insights into the functional substitutability between different types of lipids and, therefore, an improved understanding of the essentiality of a particular type of lipid, such as cardiolipin.

In this study, a cardiolipin-abundant wild-type strain and a cardiolipin-deficient strain of *R. sphaeroides* were grown in normal-phosphate and low-phosphate media and compared with respect to growth, membrane lipid profiles, and cytochrome *c* oxidase (C*c*O) expression levels. The C*c*O was purified from these two different strains under two different growth conditions and characterized in terms of UV−vis spectroscopic properties, subunit composition, and enzymatic activity. The lipid profiles of the membranes and the purified enzymes were analyzed by using quantitative ESI and MALDI MS and MS/MS, to relate the observed spectral and functional properties of C*c*O and *R. sphaeroides* to the lipid composition. The results show a striking resilience of C*c*O to dramatic changes in its lipid environment.

MATERIALS AND METHODS

Media and Growth Conditions. The cardiolipin-abundant wild-type strain, 169-2.4.1 (WT), and the CL-deficient mutant strain, 169CL3 (CL−), were grown in parallel under both phosphate-abundant (P+) and phosphate-limiting (P−) conditions. The normal-phosphate conditions included Sistrom's succinate-basal salts medium with a KH_2PO_4 concentration of 20 mM (pH 7.0) and appropriate antibiotics as described previously.[11,12] The cells were grown on agar-solidified medium or in liquid cultures at 30 °C under aerobic chemoheterotrophic conditions described in ref 13. For phosphate-limiting growth, the 20 mM KH_2PO_4 in the Sistrom's medium was replaced with 50 mM HEPES-KOH and 0.1 mM KH_2PO_4 (pH 6.8). Strain designations were as follows: WT/P+, 169-2.4.1 grown under normal phosphate; CL−/ P+, 169CL3 under normal phosphate; WT/P−, 169-2.4.1 under low phosphate; and CL−/P−, 169CL3 under low phosphate.

Isolation of *R. sphaeroides* Cell Membrane Pellets and C*c*O Purification. The C*c*O overexpressed in all *R. sphaeroides* strains (Table S1 of the Supporting Information) contained a six-histidine tag at the C-terminus of subunit II. *R. sphaeroides* cells were harvested by centrifugation in a GS-3 rotor at 14000*g* for 20 min and resuspended in pH 6.5 buffer containing 50 mM KH_2PO_4 or 50 mM Bis-Tris propane for cells grown under phosphate-limiting conditions and 1 mM EDTA. Further processing was conducted as previously described.[13] A typical yield obtained from fifteen 2.8 L Fernbach flasks of WT or CL− cell cultures was approximately 40 mg of C*c*O; under high-phosphate (P+) and low-phosphate (P−) conditions, the yields were similar. *R. sphaeroides* C*c*O was purified from isolated membrane pellets as described previously.[14]

UV−Visible Spectroscopy of a Membrane Suspension and Purified C*c*O. UV−visible optical spectra were recorded on a Perkin-Elmer Lambda 40P UV−visible spectrophotometer. For the crude membrane samples, dithionite-reduced minus ferricyanide-oxidized spectra were collected from 500 to 700 nm and the level of C*c*O was quantified by using an $\Delta\varepsilon_{606-630}$ extinction coefficient of 24 cm^{-1} mM^{-1}.[13] For the purified C*c*O samples, an absolute spectrum was measured with and without reduction with sodium dithionite from 250 to 700 nm, and the level of C*c*O was quantified by using an $\Delta\varepsilon_{606-640}$ extinction coefficient of 40 cm^{-1} mM^{-1}.[13] To counteract the acidity of the reducing agent, the samples were diluted with buffer containing 1 mM EDTA, 0.1% (m/v) dodecyl maltoside, and 100 mM HEPES (pH 7.4) prior to the analysis. At least triplicate spectra were collected for each sample.

Urea SDS−PAGE and Steady State Activity Assay of C*c*O. Sodium dodecyl sulfate−polyacrylamide gel electrophoresis (SDS−PAGE) was conducted as previously described.[15] The steady state activity of C*c*O was measured by oxygen consumption as previously described,[16] under conditions given in the figure legend.

Extraction of Lipids from Isolated Membranes. Triplicates of 20 μL of the resuspended membranes from *R. sphaeroides* cells (diluted with water to a protein concentration of 1 mg/mL determined by the BCA assay) were freeze-dried, and lipids were extracted by sequential addition of 2 × 50 μL of a chloroform/methanol mixture (2:1, v/v), 1 × 50 μL of an ethyl ether/methanol mixture (1:1, v/v), and 2 × 50 μL of a chloroform/methanol/ammonium hydroxide mixture (100:50:2, v/v/v) followed by vigorous vortexing.[17] The extracts were combined, dried under vacuum, and redissolved in 50 μL of a chloroform/methanol mixture (1:1, v/v) prior to mass spectrometry analysis.

Identification of Lipids Using ESI MS and CID MS^n. Mass spectrometric analyses of lipids were performed using a model LTQ linear quadrupole ion trap (Thermo Fisher Scientific, San Jose, CA), equipped with a nanoelectrospray ionization source (ESI) for analysis of membrane lipid extracts, and a Thermo model LTQ-XL linear ion trap mass spectrometer equipped with a vacuum matrix-assisted laser desorption ionization source (vMALDI) for direct analysis of membranes and purified enzymes. The total lipid extracts obtained as described above were diluted 4-fold using a $CHCl_3/CH_3OH$ mixture (1:1, v/v) containing 40 mM ammonium hydroxide and introduced into the mass spectrometer by direct infusion through noncoated silica tips with internal diameters of 30 μm (New Objective, Inc., Woburn, MA), at a flow rate of 0.5 μL/min. NanoESI conditions were optimized to maximize the sensitivity and stability of the precursor ions of interest while minimizing "in-source" fragmentation. Typical nanoESI conditions were as follows: heated capillary temperature, 180 °C; spray voltage, 1.8 kV; capillary voltage, 20 V (−20 V for negative ion mode); tube lens voltage, 75 V (−75 V for negative ion mode). Mass spectra (MS) were acquired from m/z 150 to 2000 using the enhanced scan mode.

Collision-induced dissociation (CID) tandem mass spectrometry (MS/MS) and multistage tandem mass spectrometry (MS^n) experiments were performed by using helium as the collision gas and an activation time of 30 ms in the linear ion trap. Collision energies were optimized for each precursor ion of interest. Typically, an activation q value of 0.2 was used to achieve a reasonable low-mass cutoff while still maintaining good sensitivity. Depending on the activation q values, the corresponding optimal normalized collision energies applied were typically 25% for the phospholipids,

ornithine lipids, and glutamine lipids and increased to 40% for SQDG lipids. The isolation width for obtaining isotopical isolation of precursor ions was typically 1.2 Da for protonated and deprotonated ions and 1.5−2.0 Da for noncovalent cationic or anionic adduct ions.[18] The spectra shown were typically the average of 50−300 scans. Each scan was typically an average of three microscans. The target number was set at 1×10^4 for MS and 3×10^4 for MS^n. For the identification analysis, the maximal injection time was typically set at 50 ms for both MS and MS^n. For comprehensive lipid identifications, lipid precursor ions with normalized relative abundances higher than 1% in MS were further examined by MS/MS and MS^n manually and in automatic acquisition mode. The structures of lipids were determined by comparing the MS/MS and MS^n spectra with those of available standards or by rationalizing on the basis of knowledge of the gas-phase fragmentation behaviors of the lipid.[1,19−21]

Quantification of Lipids using ESI MS and CID MS/MS. Total lipid extracts from each membrane sample were diluted 4-fold using a $CHCl_3/CH_3OH$ mixture (1:1, v/v) containing ammonium hydroxide at a final concentration of 40 mM and mixed with internal standards PE 14:0/14:0, PG 14:0/14:0, PC 14:0/14:0, and $CL(14:0)_4$ at final concentrations of 4, 2, 2, and 1 μM, respectively, followed by sample infusion for ESI analysis. At least triplicate independent extractions were performed, and each MS spectrum was an average of 100−250 scans, each containing three microscans, acquired from m/z 150 to 2000 in both positive and negative ion modes. The MS spectra were processed by Gaussian 5 point smoothing and corrected for chemical baseline noise, isotopic distributions, and isotopic overlapping. Intensities of all the ions in the processed spectra of each sample were first normalized to the internal standards observed in MS and then converted into the quantity (for phospholipids with available standards) or relative quantity (lipids without standards of the same headgroup) of each lipid species using independently generated external calibration curves.[21]

Extensive MS/MS quantification experiments of lipid extracts were conducted using automatic acquisition. For all the peaks with normalized relative abundances in MS of >10% in the m/z range of 600−1600, MS/MS spectra of isotopically isolated precursor ions (isolation width of 1.2 Da for singly charged ions and 0.8 Da for doubly charged ions) were recorded with 50 ms maximal injection times and under an MS/MS target number of 3×10^4 and an activation q value of 0.2. For all the peaks above 1% but equal to or below 10% as well as all the internal standards again, the maximal injection time was increased to 100 ms, and the number of scans collected was increased to ~4-fold higher than those at >10% relative abundance whenever possible. Each scan was the average of three microscans. The normalized collision energy applied was 30% for positive ion mode and 25% for negative ion mode. Isolation and MS/MS activation of singly charged CL precursor ions using isolation widths of 10 Da were conducted using automatic acquisition, and the characteristic product ions at m/z 699 for $CL(18:1)_4$ and m/z 591 for the internal standard $CL(14:0)_4$ were used for CL quantification. MS/MS spectra of all the SQDG species using normalized collision energies of 35% were also acquired automatically using a maximal injection time of 100 ms, regardless of the abundance in the MS spectra. These experiments were all performed on triplicate extraction samples. Quantification was based on the relative abundance ratios of primary product ions from each lipid over the lipid internal standards.

Direct Lipid Identification Using MALDI-LIT MS and MS^n. Direct MS and MS^n analyses of isolated membranes and purified C*c*O were performed via vMALDI-LIT. One microliter of either resuspended membrane (at a protein concentration of 0.25 mg/mL determined by the BCA assay using bovine serum albumin as the standard) or 1 μL of purified C*c*O (25 μM) was applied to individual spots on the stainless steel MALDI sample plate and dried in air, followed by application of 1 μL of 0.1 M (for membrane samples) or 0.5 M (for purified enzymes) 2,5-hydroxybenzoic acid (2, 5-DHB) dissolved in an acetonitrile/water mixture (2:1, v/v). MS and MS/MS spectra were recorded in negative and positive ion modes using enhanced resonance ejection scan conditions. The typical optimal laser power setting was 20 for positive ion mode analyses and 30 for negative ion mode analyses. MS spectra were recorded at m/z 200−2000. CID MS/MS and MS^n spectra were recorded at a normalized collision energy of 30%, an isolation width of 1.2 or 1.5 Da to achieve isotopical isolation, and an activation q of 0.2. The MALDI spectra shown were the average of 250 scans. The MALDI MS spectra were processed by Gaussian 5 point smoothing and corrected for chemical baseline noise prior to relative quantification of CL by using MS peak heights.

Direct Relative Quantitative Lipid Analysis Using MALDI-LIT MS. An internal standard mixture containing PE 14:0/14:0, PG 14:0/14:0, PC 14:0/14:0, and $CL(14:0)_4$ at final concentrations of 10, 5, 1.25, and 1.25 μM, respectively, in methanol was added to the membrane suspension (final protein concentration of 0.25 mg/mL) or the purified C*c*O solution (final C*c*O concentration of 4.2 μM, i.e., protein concentration of 0.5 mg/mL) to form one-phase mixtures. One microliter of each mixture was then applied to the vMALDI plate and processed as described above.

RESULTS AND DISCUSSION

Cell Growth, C*c*O Production, and Purification Stability. No obvious difference in the cell culture optical density at harvest was observed between the WT and CL− strains grown under phosphate-abundant or phosphate-deficient conditions. The UV−vis spectroscopic analysis of the isolated membranes also shows very similar spectral characteristics for all of these four samples, and no shift in the absorption peak at 606 nm (heme *a*) was observed (Figure 1A). These findings indicate that all four conditions can produce similar amounts of C*c*O, and that the C*c*O produced has native structure in the membrane, as indicated by the unaltered spectral characteristics, even when both CL deficiency and phosphate deficiency are imposed. The purification profiles of C*c*O from Ni-NTA FPLC are also very similar for these four samples, in terms of the peak elution conditions, the relative abundances of the eluted protein peaks (data not shown), and the purification yields. It appears that neither the CL deficiency, the phosphate deficiency, nor the combination affects the production, the metal center assembly, or the stability of the multisubunit protein complex during enzyme purification.

UV−Vis Spectroscopic Properties of the Purified C*c*O. The reduced spectra of the purified C*c*O from the four samples (Figure 1B) display no appreciable difference in the absorption wavelength of the peaks or the relative intensities between the Soret (445 nm) and α heme a/a_3 (606 nm) absorption peaks. The fact that no peak shift is observed indicates that the coordination states of the heme *a* and heme a_3-Cu_B catalytic centers are not disturbed in the final purified C*c*O by these P+ or P− growth conditions.

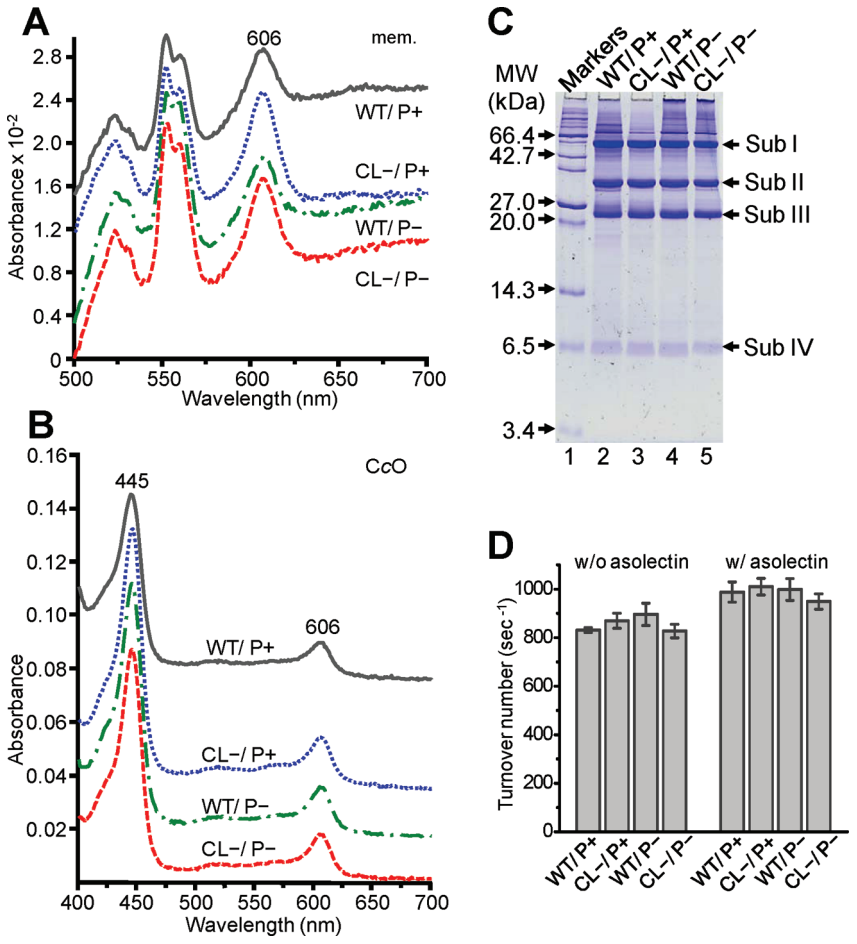

Figure 1. Expression and activity of C*c*O from *R. sphaeroides*. (A) Reduced minus oxidized UV−vis spectra of the resuspended membranes from the four different conditions showing the native spectral band at 606 nm and the high level of expression (peak height at 606 nm vs 560 nm). (B) Absolute spectra of C*c*O purified from these membranes by Ni^{2+}-NTA FPLC showing the identical peak positions at 445 and 606 nm indicating that the purified C*c*O forms all have native spectral characteristics. (C) SDS−PAGE of purified C*c*O showing the four subunits normally seen in *R. sphaeroides* C*c*O. The fainter molecular weight bands above the major band of subunit I reflect a polymerization artifact that occurs during the sample preparation for the SDS gel. (D) Steady state oxygen consumption activity analysis of the purified C*c*O species measured in 30 μM cytochrome *c*, 1 mM TMPD, 2.8 mM ascorbic acid, and 0.05% dodecyl maltoside in 50 mM KH_2PO_4 (pH 6.5) buffer with and without asolectin lipids [final concentration of soybean asolectin of 1.1 mg/mL and final concentration of cholate of 0.02% (m/v)]: gray for WT/P+, blue for CL−/P+, green for WT/P−, and red for CL−/P−. None of the enzymes alone (nor cytochrome *c* alone) had a significant oxidation rate in the assay buffer system, indicating a specific cytochrome *c* oxidase reaction.

SDS−PAGE Analysis of the Purified C*c*O. SDS−PAGE analysis of the four versions of purified C*c*O (Figure 1C) clearly shows that they each contain all of the four subunits, and there is no observable difference between the four samples in terms of subunit composition or the size of the subunits that can be resolved via SDS−PAGE. An FPLC peak that eluted earlier than the pure C*c*O contained other respiratory complexes such as a cytochrome bc_1 (Complex III) that also appeared unaffected by the P− growth conditions or the CL−- mutation (data not shown). Importantly, the combination of phosphate and cardiolipin deficiencies did not cause the C*c*O subunits to dissociate from each other during purification, because the yield of the purified enzyme was similar in all cases. This is particularly intriguing with respect to subunit IV, because it is connected to the rest of the enzyme via four phospholipid molecules identified as PE in the four-subunit *R. sphaeroides* C*c*O crystal.[22]

Activity Analysis of the Purified C*c*O. The steady state activities (oxygen consumption) of the C*c*O from these four samples are similar (Figure 1D). The addition of soy asolectin, a lipid mixture containing PE, PC, phosphatidylinositol (PI), phosphatidic acid (PA), lysoPC, and other unspecified lipids (Avanti Polar Lipids Inc., Alabaster, AL), in the assay increases the activity by 20−30% for all samples, which is typical for purified oxidase produced under normal conditions.

Thus, the phosphate-limiting growth condition and the combination of the phosphate-limiting growth and the genetic CL deficiency do not affect the UV−vis spectroscopic properties, the subunit composition, the activity of the purified C*c*O enzymes, or the C*c*O expression level (milligrams of C*c*O protein per milligram of total membrane protein; P+ growth, 3.7 ± 1.1%; P− growth, 3.4 ± 0.9%). However, the lipid profiles in the cells are expected to have changed.[1] To address the extent and nature of the changes, we examined the lipid profiles in the membrane and in the purified C*c*O enzymes by quantitative ESI and MALDI MS and MS/MS methods with the incorporation of internal lipid standards.

Membrane Lipid Analysis by Quantitative MS. Figure 2A shows the positive ion mode ESI MS spectra (m/z 600−1000) of

dx.doi.org/10.1021/bi1017039 |*Biochemistry* 2011, 50, 3891–3902

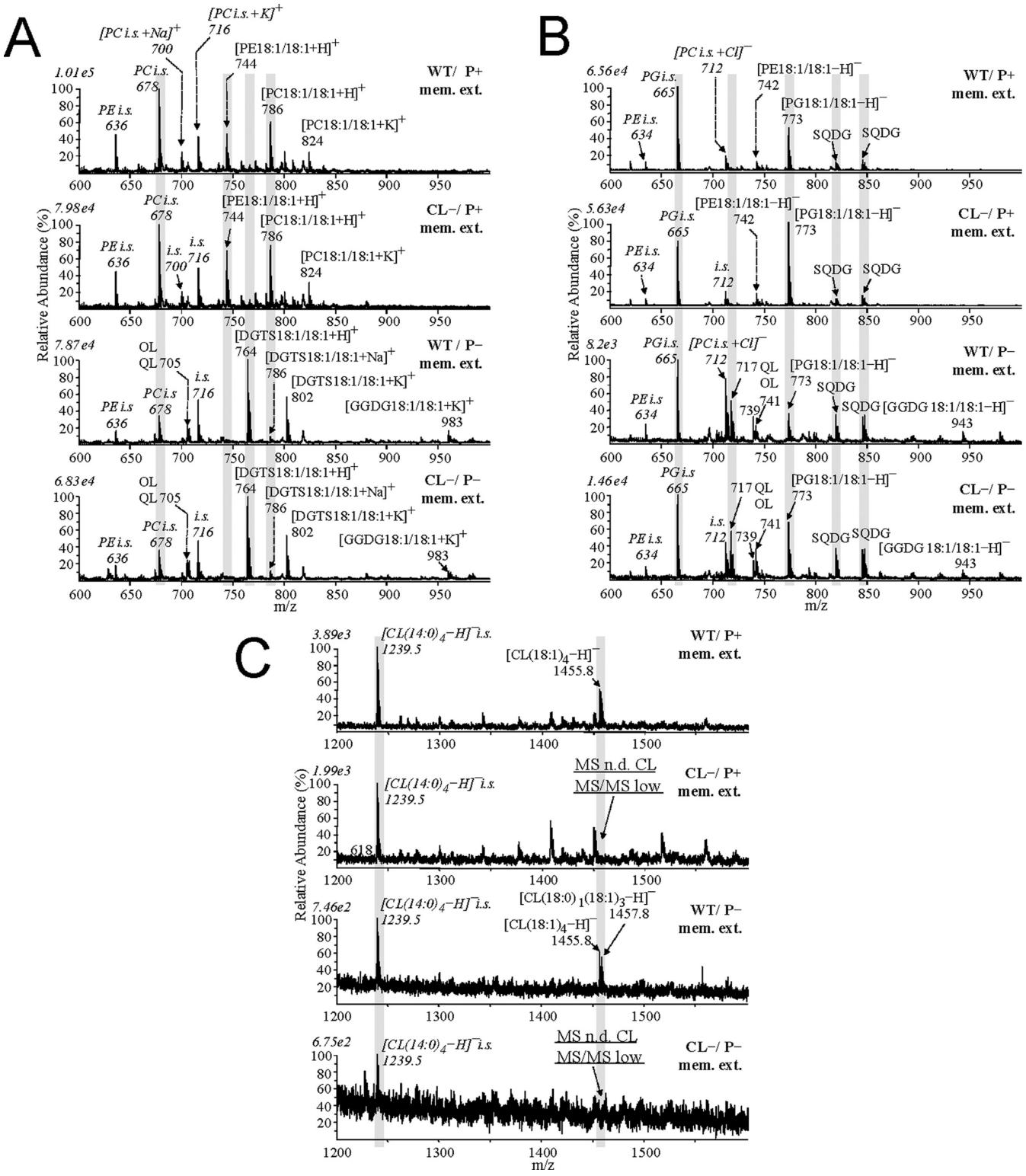

Figure 2. ESI MS spectra of membrane extracts (mem. ext.) from the same amount of isolated membranes of *R. sphaeroides* strains WT/P+, CL−/P+, WT/P−, and CL−/P− prepared as described in Materials and Methods. The data show the marked changes in lipid species in response to the *cls* mutation and the phosphate-limited growth conditions. Species that exhibit alterations are highlighted, in particular, the loss of CL at m/z 1455.8 in CL−/P− membranes: (A) positive ion mode, (B) negative ion mode (m/z 600−1000), and (C) negative ion mode (m/z 1200−1600). Phospholipid internal standards are labeled as i.s. and include PE (m/z 636) and PC (m/z 678) in positive ion mode (A), PE (m/z 634), PG (m/z 665), and PC+Cl (m/z 712) in negative ion mode (B), and CL (m/z 1239.5) in negative ion mode (C). The percent relative abundance scale shows numbers above the *Y*-axis that give the absolute abundance of the most abundant peak to which the other peaks are scaled; e.g., 1.01×10^5 indicates the absolute ion count of the most abundant peak (PC i.s. at m/z 678) is 10100. The data are quantified on the basis of relative peak heights compared to internal standards. The results of the quantification are summarized in Figure 3 and Tables 1 and 2.

dx.doi.org/10.1021/bi1017039 |*Biochemistry* 2011, 50, 3891–3902

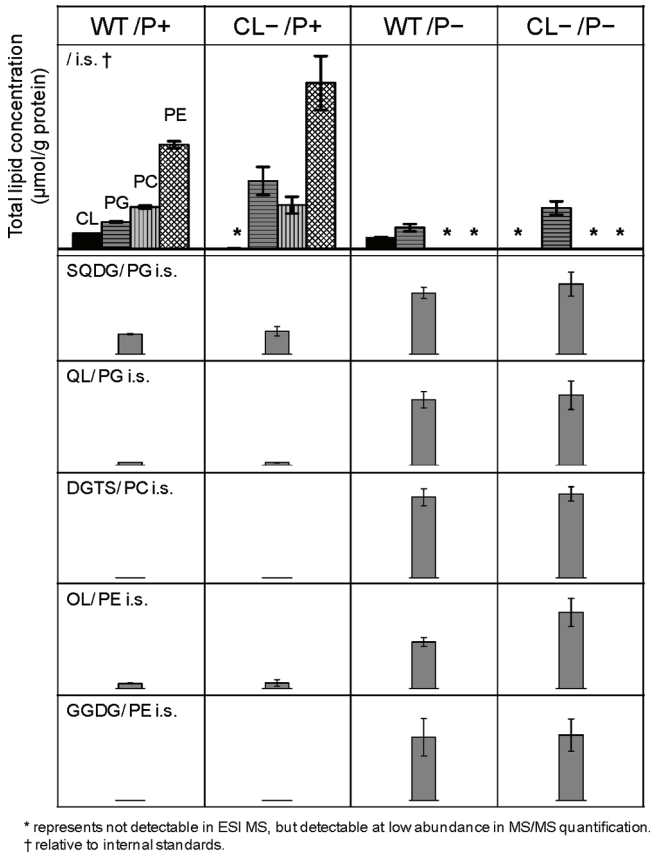

Figure 3. Summary of quantification of the membrane lipids in WT/P+, CL−/P+, WT/P−, and CL−/P− using ESI MS following lipid extraction. The total content of each lipid in micromoles per gram of protein is calculated on the basis of known amounts of internal standards for CL, PG, PC, and PE, and known amounts of protein, as described in Materials and Methods. Where no standard is available, the closest related chemical structure was used to give a relative change in SQDG, QL, DGTS, OL, and GGDG. These non-phospholipids all exhibited significant apparent increases compared to the diminished levels of the phospholipids under P− growth. More detailed analysis of the lipid species is presented in Table 1.

the lipids extracted from the resuspended membrane pellets obtained from the four different conditions: WT/P+, CL−/P+, WT/P−, and CL−/P−. Phosphate limitation causes more radical changes in MS lipid profiles than CL limitation alone, as seen for WT/P+ versus WT/P−, compared to WT/P+ versus CL−/P+ . None of the PC and PE lipids predominant in WT/P+ can be observed in WT/P−, which is now dominated by a new set of lipids. The identities of the lipid species were determined by using MS/MS and MS^n (data not shown). The most abundant ion observed for WT/P− at m/z 764 was determined to be the protonated ion of DGTS (*N*,*N*,*N*-trimethylhomoserine diacylglycerol) 18:1/18:1, a polar non-phospholipid that carries a fixed positive charge in the headgroup (Scheme S1 of the Supporting Information). It also forms a sodium adduct ion at m/z 786, the same m/z value as that of the protonated ion of PC 18:1/18:1, but MS/MS analysis of the ion at m/z 786 revealed that it contains only a very low level of PC (product ion at m/z 184) and is predominantly the sodium adduct ion of DGTS. Another type of phosphate-free lipid, glucosylgalactosyldiacyllglycerol, GGDG (Scheme S1 of the Supporting Information), was also observed in the P− growth membranes. Similar drastic lipid profile changes are observed between CL−/P+ and CL−/P− in the positive ion mode MS spectra. CL deficiency by itself does not cause such major changes in the lipid species seen in positive ion mode MS (Figure 2A), because the main differences are in the levels of cardiolipin itself and other lipids containing negatively charged headgroups, which are typically not seen in the positive ion mode.

Figure 2A (panels 3 and 4) shows that during P− growth, regardless of whether CL is deficient, PC or PE lipid ions do not reach beyond 5% of the normalized relative abundance in MS, and the abundance of DMPE, the intermediate in making PC from PE, also drops to below 5%. In their place, there is an increased level of OL, and the appearance of high levels of DGTS and GGDG lipids. The most abundant fatty acid composition for DGTS is DGTS 18:1/18:1. Correspondingly, the DGTS and GGDG lipids cannot be detected in the P+ growth conditions (Figure 2A, panels 1 and 2). Under P+ growth, the CL− mutant has a slightly higher level of PE lipids than the WT, but under P− growth, the CL− mutant does not show an appreciably higher level of OL than WT, although OL has been described as being functionally substitutable with PE.[1,3] Both WT and CL− strains show similar high levels of DGTS and GGDG under P− growth, and similar levels of PC under P+ growth.

The negative ion mode ESI MS spectra of the lipids extracted from these four membrane samples are shown in Figure 2B (m/z 600−1000). PC and PE are not strongly detected in negative ion mode MS, but the PG lipids are observed at measurable levels under P+ and P− growth in both the WT and the CL− strains. Appreciable increases in the levels of other types of non-phospholipids are also observed. Among these is the peak at m/z 717 in Figure 2B (panels 3 and 4), which is determined to be mainly the glutamine lipid QL 3-OH 20:1/18:1 with a low level of overlapping OL 3-OH 20:1/19:1. This is the first time that the recently discovered glutamine lipid has been found to change under different growth conditions.[20,21] The relative abundance of the SQDG ions also increases in P−.

Results of quantification of the lipid species resolved in negative ion mode MS by using phospholipid internal standards are summarized in Table 1 [with the exception of those for CL (see below)]. SQDG, QL, and GGDG lipids are relatively quantified by comparison to the PG internal standard, and OL, MMPE, and DMPE lipids are relatively quantified by comparison to the PE standard. P− growth causes the levels of PG lipids, including PG 18:1/18:1 and PG 18:0/18:1, to decrease by ∼50% in both WT and CL− strains. However, the level of PG 18:0/18:0, containing two fully saturated fatty acids and barely observable under P+ growth, increases under P− growth for both WT and CL− strains. P− growth also caused the levels of SQDG lipids, both saturated and unsaturated molecular species, to increase by 2−3-fold for both WT and CL− strains. The levels of QL lipids increased dramatically (>5-fold) in P− growth, and the increase for QL 3-OH 20:1/18:1 (m/z 717) is slightly more appreciable in CL− than in WT.

Figure 2C shows the m/z 1200−1600 regions of the negative ion mode ESI MS spectra in which singly deprotonated CL ions are detected. In membrane lipid extracts from WT/P−, the level of cardiolipin decreases by only ∼20% compared to its level in WT/P+, while in CL−/P+, the level of cardiolipin is already below the ESI MS detection limit. Thus, quantification of CL requires CID MS/MS fragmentation at m/z 1455.8 [$CL(18:1)_4$] and m/z 1239.5 [$CL(14:0)_4$ internal standard] precursor ions. The results are summarized in Tables 1 and 2. All of the lipid ions

Table 1. Quantification of Membrane Lipids Using ESI MS and MS/MS[a]

lipid type	lipid species	WT/P+	CL−/P+	WT/P−	CL−/P−	method
CL	CL 18:1	7.69 ± n/a[b]	0.43 ± 0.09	5.64 ± 0.36	0.05 ± 0.00	**absolute**
PG	PG 18:1/18:1	10.9 ± 0.3	28.3 ± 5.9	6.9 ± 0.6	14.6 ± 2.3	
	PG 18:0/18:1	2.0 ± 0.0	4.3 ± 0.9	1.9 ± 0.4	4.1 ± 0.9	
	PG 18:0/18:0	0	0.3 ± 0.0	0.7 ± 0.3	0.8 ± 0.1	
	PG 18:1/19:1	0.5 ± 0.0	0.9 ± 0.2	1.1 ± 0.6	0.9 ± 0.1	
PE	PE 18:1/18:1	44.0 ± 1.4	71.1 ± 11.1	0	0	
	PE 18:0/18:1	7.8 ± 0.3	11.1 ± 2.4	0	0	
PC	PC 16:0/18:0	1.2 ± 0.1	1.1 ± 0.2	0	0	
	PC 18:1/18:1	13.3 ± 0.3	15.4 ± 2.8	0	0	
	PC 18:0/18:1	1.4 ± 0.2	1.6 ± 0.5	0	0	
	PC 18:1/19:1	4.9 ± 0.2	3.7 ± 0.7	0	0	
SQDG	SQDG 16:0/16:0	0.8 ± 0.0	0.5 ± 0.1	2.3 ± 0.3	2.8 ± 0.4	**relative**
	SQDG 16:0/18:1	2.2 ± 0.1	2.3 ± 0.6	7.4 ± 0.6	8.0 ± 1.1	
	SQDG 16:0/18:0	1.1 ± 0.1	1.1 ± 0.1	2.6 ± 0.4	3.4 ± 0.7	
	SQDG 18:1/18:1	2.9 ± 0.1	3.6 ± 0.9	7.3 ± 0.6	8.1 ± 1.2	
	SQDG 18:0/18:1	1.4 ± 0.0	2.0 ± 0.4	5.9 ± 0.3	6.7 ± 1.3	
	SQDG 18:0/18:0	0.3 ± 0.0	0.3 ± 0.0	0.8 ± 0.3	1.1 ± 0.5	
OL	OL 3-OH 18:0/19:1	0	0	0	27.6 ± 1.9	
	OL 3-OH 18:1/20:2, OL 3-OH 18:0/20:3	0	0	0	27.5 ± n/a[b]	
	OL 3-OH 20:1/18:1	4.0 ± n/a[b]	2.4 ± 6.0	53.6 ± 6.3	66.8 ± 15.3	
	OL 3-OH 20:0/18:1, OL 3-OH 20:1/18:0	0	0			
	OL 3-OH 20:1/19:1	8.5 ± 1.3	11.0 ± 2.2	25.6 ± 1.0	26.1 ± 6.9	
	OL 3-OH 20:0/21:1	1.7 ± 0.4	0	0		
QL	QL 3-OH 20:1/18:1 mainly, OL 3-OH 20:1/19:1	0.7 ± 0.1	0.7 ± 0.1	11.8 ± 1.6	12.3 ± 2.4	
	QL 3-OH 20:0/18:1 mainly	0	0	5.8 ± 0.5	6.5 ± 1.4	
DGTS	DGTS 18:1/18:1	0	0	63.0 ± 6.9	66.0 ± 5.7	
	DGTS 18:0/18:1	0	0	23.5 ± 2.2	24.1 ± 2.0	
GGDG	GGDG 18:1/18:1+K	0	0	27.4 ± 8.1	28.3 ± 7.0	
MMPE, DMPE, PE	MMPE 18:1/18:1, PE 19:1/18:1, PE 18:1/19:1	7.9 ± 0.5	8.8 ± n/a[b]	8.3 ± n/a[b]	8.5 ± n/a[b]	
	MMPE 18:1/19:1, MMPE 19:1/18:1, DMPE 18:1/18:1, PE 18:1/20:1, PE 20:1/18:1	12.0 ± 4.6	9.9 ± 2.4	0	0	
	DMPE 18:1/18:1	10.6 ± 0.9	16.7 ± 4.9	0	0	

[a] The quantities of lipids are represented in micromoles of lipid per gram of membrane protein. Amounts of phospholipids CL, PG, PE, and PC are represented as absolute quantities, and the other lipids without internal standards are quantified with respect to the most related internal standards (OL, MMPE, DMPE, GGDG/PE i.s., QL/PG i.s., SQDG/PG i.s., and DGTS/PC i.s.) for relative comparisons following isotopic corrections. Values represent the means ± systematic errors calculated from the standard deviation of at least three independent extractions. [b] Error not available.

above 5% normalized relative abundance in MS have been quantified by MS/MS in these samples (Figure 3 and Table 1). Because CL can often be substituted with PG and PG has been shown to functionally exchange with SQDG, the quantification of CL (by MS/MS) and PG (by MS) and the relative quantification of SQDG lipids (by MS) are all included in Table 1. The MS/MS quantification of CL clearly indicates that the level of cardiolipin in the CL− mutant was further decreased by the P− growth, and a 5-fold "cleaner" CL-deficient membrane sample is obtained through the combination of the CL-deficient mutation and P− growth [CL−/P−, 0.05 μmol of CL/g of protein (0.7% of WT/P+); CL−/P+, 0.43 μmol of CL/g of protein (5.5% of WT/P+) (Tables 1 and 2)]. Second, WT/P− membranes maintain 73% of the cardiolipin level in WT/P+. This is in stark contrast to PE and PC, which are found to be nearly completely depleted by P− growth. These results suggest that with limited phosphate growth, the highest priority is CL (73% maintained), followed by PG (50% maintained), whereas PE and PC have the lowest priority (Table 2).

While the levels of both PG and CL decrease under P− growth, the level of the non-phospholipid SQDG increases significantly. Because all of the SQDG, PG, and CL lipids carry a negative charge and are also capable of forming hydrogen bonds in the headgroup under physiological conditions, this observation is likely due to the cells' compensatory response to maintain the total amount of negative charge at a certain level to meet their physiological needs.[2] This suggests that what matters in these lipids is the negatively charged center supplied by carboxylic acid or sulfite groups, usually supplied through phosphate groups. The nearly complete depletion in PC and the concomitant dramatic increase in DGTS, both lipids containing a zwitterionic center carrying a fixed positive charge in the tetra-alkyl amino group, however, suggest that the theme of a zwitterionic center containing a fixed positive charge is also important. The negatively charged phosphate group in PC

dx.doi.org/10.1021/bi1017039 |*Biochemistry* 2011, 50, 3891–3902

Table 2. Comparison of ESI and MALDI Analysis of CL Content in the Membrane and Purified C*c*O from P+ and P− Growth of the WT and CL− Mutant

	sample	membrane	C*c*O
ESI	WT/P+	100%[a]	n/a[d]
MS/MS	CL−/P+	5.5 ± 1.1%	n/a[d]
	WT/P−	73.3 ± 4.7%	n/a[d]
	CL−/P−	0.7 ± 0%	n/a[d]
MALDI	WT/P+	100%[b]	100%[c]
	CL−/P+	12 ± 4%	27 ± 3%
	WT/P−	53 ± 18%	74 ± 14%
	CL−/P−	MS n/d[d]	MS n/d[d]

[a] Representing an absolute value of 7 μmol of lipid/g of membrane protein (see Table 1). [b] Representing 12.5 μmol of lipid/g of membrane protein relative to a single internal standard. [c] Representing 5.3 μmol of lipid/g of C*c*O protein. [d] n/d, not detected; n/a, not available.

can be replaced with the carboxylic acid group in DGTS. Because a similar charge center can be provided by the non-phospholipid, the limited phosphate resource is not required to make PC.

Thus, in spite of the close-to-wild-type level of expression and properties of the C*c*O protein under all four conditions, limited phosphate in the growth medium causes drastic changes in the membrane lipid profiles of both the WT and the CL− mutant *R. sphaeroides*. In particular, the combination of the CL− mutation with P− growth creates a significantly more depleted CL-deficient strain than the mutation alone [companion paper (DOI 10.1021/bi101702c)]. The ESI results discussed so far are obtained from the lipid extracts of *R. sphaeroides* membranes in the absence of detergents. To improve our understanding of the potential role of CL in *R. sphaeroides* C*c*O, we were forced to look at the lipids that are associated with detergent-purified C*c*O, which can be performed more readily using MALDI.

MALDI Analysis of Lipids in Membranes and Purified C*c*O. Because of the interference from detergents and potential issues associated with incomplete chemical extraction for ESI MS analysis of lipid extracts from the purified C*c*O, direct MALDI MS and MS/MS were applied in performing relative quantification of the lipids in the purified C*c*O, by incorporating a set of internal standards at appropriate concentrations in the enzyme solution. For comparison, the same methods were also applied to direct analysis of the resuspended membrane pellets, and the results were compared to those obtained by ESI on the membrane lipid extracts.

Both MALDI and ESI analyses lead to similar conclusions with regard to the relative quantitative changes in the membrane lipids observed as a result of the CL− mutation and/or P− growth. Figure 4A shows the direct MALDI MS spectra of the membranes from WT/P+, CL−/P+, WT/P−, and CL−/P− *R. sphaeroides* in the positive ion mode. Under P− growth (Figure 4A, panels 3 and 4), DGTS is the predominant species observed in positive ion mode and PC is nearly completely depleted, consistent with the ESI analysis. Likewise, negative ion mode MALDI MS (Figure 4B, panels 3 and 4) also reveals the partial retention of PG lipids and an increase in the level of SQDG (relative to the PG internal standard), particularly in the saturated SQDG species, in response to the phosphate depletion during P− growth. The *m/z* 1200−1600 region of the negative ion mode MALDI MS spectrum (Figure 4C) shows that cardiolipin can be detected at 53% in WT/P− and at 12% in CL−/P+, compared to WT/P+ (Table 2), but cannot be detected in CL−/P−, suggesting CL−/P− has much less cardiolipin. Also noticeable is the fact that the MALDI MS analysis shows more sensitivity for the detection of cardiolipin compared to ESI under the conditions applied here. The comparison of the MALDI MS analysis directly on the membranes with the ESI MS and MS/MS analyses on the membrane lipid extracts shows that the direct MALDI analysis method gives valid quantitative results through incorporation of lipid internal standards, optimization of experimental conditions, and running multiple replicates of experiments. MALDI is also advantageous in that it is less affected by high levels of detergent in purified enzyme solutions.

Despite the presence of abundant adduct ions unrelated to lipid species (as determined by control experiments), the purified C*c*O from the four different conditions could be analyzed by direct quantitative MALDI MS by comparison with phospholipid internal standards, as shown in Figure 5. In the positive ion mode MS under P+ growth (Figure 5A, panels 1 and 2), the phospholipid PC 18:1/18:1 (protonated ions and sodium adduct ions) is observed as the major lipid species of the purified C*c*O from both WT/P+ and CL−/P+. Although known to be present in the purified WT/P+ C*c*O, PE lipid peaks are not observed likely because of their suppressed ionization efficiency in MALDI in the presence of PC and detergents. Heme *a* from the catalytic center (structure confirmed by MS/MS at *m/z* 852 and 835) is clearly observed in MS at a high ion abundance for all four C*c*O samples. Under P− growth (Figure 5A, panels 3 and 4), C*c*O from WT/P− and C*c*O from CL−/P− display no detectable PC (*m/z* 786 and 808), while the non-phospholipid DGTS 18:1/18:1 becomes a more abundant lipid ion (*m/z* 764; identified by MS/MS). The negative ion mode MS spectra show that under P+ growth (Figure 5B, panels 1 and 2), PG 18:1/18:1 and a series of SQDG lipids are retained in the purified C*c*O from WT/P+ and CL−/P+. By comparison to the PG internal standard at *m/z* 665, CL−/P+ C*c*O shows an increased level of PG 18:1/18:1 compared to WT/P+ (*m/z* 773). However, under P− growth (Figure 5B, panels 3 and 4), C*c*O from WT/P− still contains PG 18:1/18:1 at ∼50% of its level in WT/P+, while in the CL−/P− sample, the level decreases and cannot be detected in the MS spectra. SQDG lipids are observed in both WT/P− and CL−/P− C*c*O samples. These general trends of lipid changes seen in the purified C*c*O are consistent with those seen in the membranes by both ESI (Table 1) and MALDI (Table 2).

The changes in cardiolipin in the four versions of purified C*c*O are shown in the *m/z* 1200−1600 region of the negative ion mode MALDI MS spectra (Figure 5C). In the WT/P+ C*c*O (Figure 5C, panel 1), several cardiolipin species are detected, including the most abundant $CL(18:1)_4$ at *m/z* 1455.8 and the less abundant $CL(16:0)_1(18:1)_3$ at *m/z* 1429.8. A predominant cardiolipin species found in mammalian heart, $CL(18:2)_4$ (expected at *m/z* 1448.8), is notably not present in any of the *R. sphaeroides* C*c*O species. The negatively charged sodium- and potassium-adducted ions of $CL(18:1)_4$ are also formed at *m/z* 1478.9 and 1494.9, respectively. The abundant ions at *m/z* 1495.8 and 1497.8 displayed characteristic fragmentation behaviors in MS/MS and MS^n that are not related to cardiolipin lipids or any known phospholipids. The level of cardiolipin in the purified enzyme from the CL−/P+ condition is significantly reduced compared to that of internal standard $CL(18:1)_4$: $CL(14:0)_4$ can be observed at 27% of the level in WT/P+ C*c*O. This is higher than the value of 12% seen in the membrane of CL−/P+. Under P− growth (Figure 5C, panels 3 and 4), the WT/P− C*c*O still contains

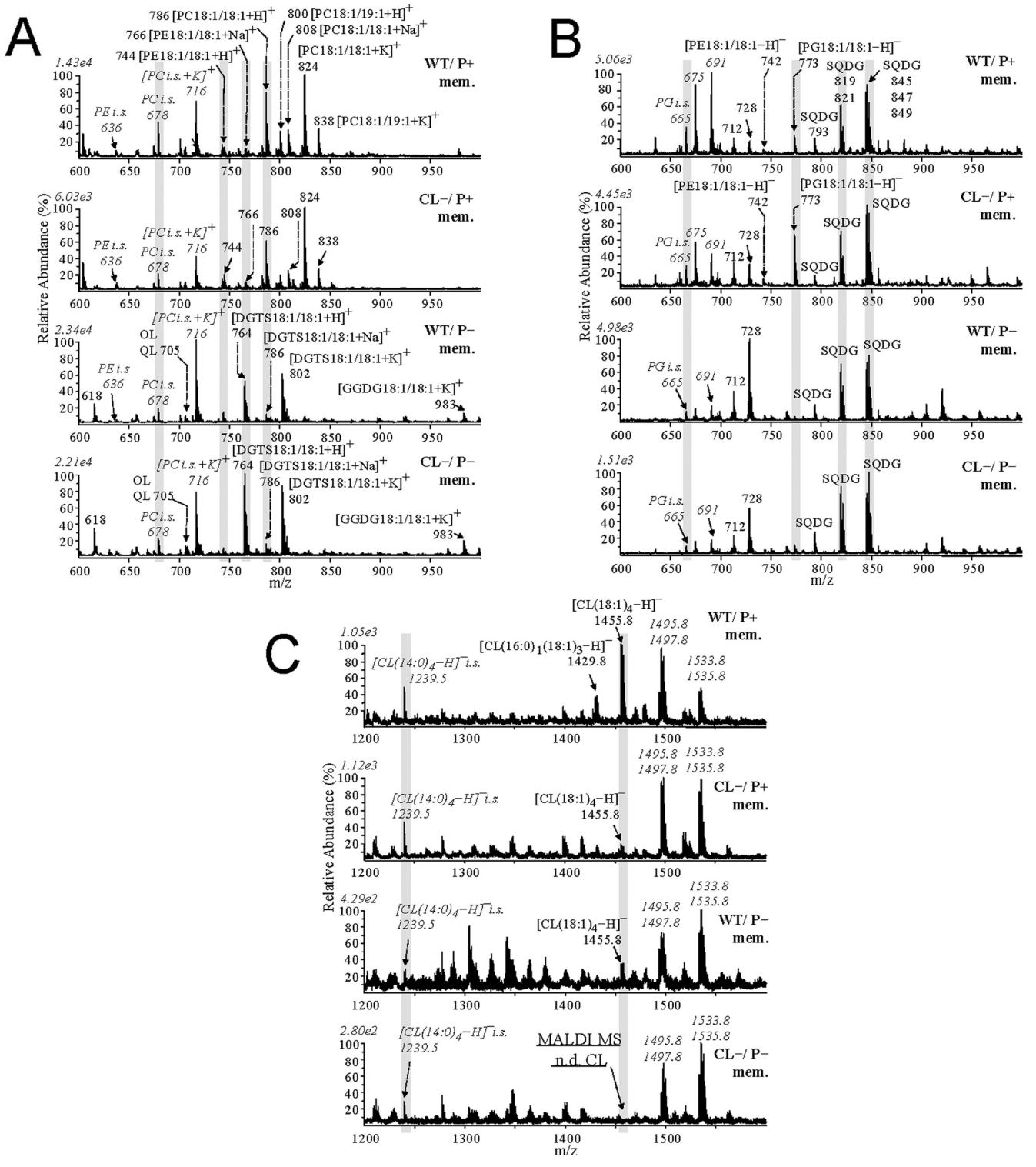

Figure 4. Direct MALDI MS quantification of lipids relative to phospholipid internal standards (i.s.) in the unextracted isolated membranes (mem.) from *R. sphaeroides* strains under different growth conditions as described in Materials and Methods. WT/P+, CL−/P+, WT/P−, and CL−/P− in (A) positive ion mode, (B) negative ion mode at *m/z* 600−1000, and (C) negative ion mode at *m/z* 1200−1600. The highlighted peaks emphasize internal standards and lipids of interest. In panel A under P− conditions, there is loss of PC (*m/z* 286, 824, and 838) and gain of DGTS (*m/z* 802), while in panel B under P− conditions, there is relative loss of PG (*m/z* 773) and retention of SQDG (*m/z* 819, 821, 845, 847, and 849). In panel C under P− conditions, loss of CL (*m/z* 1455.8 and 1429.8) is seen relative to the CL internal standard (*m/z* 1239.5). The negative ion mode peaks at *m/z* 1495.9, 1497.9, 1533.8, and 1535.8 were determined by MS/MS and MS^n not to be CL or CL derivatives.

~74% of the cardiolipin level in the WT/P+ CcO, similar to the cardiolipin levels and species in the corresponding membranes. In contrast, the CL−/P− CcO contains such a low level of cardiolipin that no $CL(18:1)_4$ ions can be detected by MALDI MS, also

dx.doi.org/10.1021/bi1017039 |*Biochemistry* 2011, 50, 3891–3902

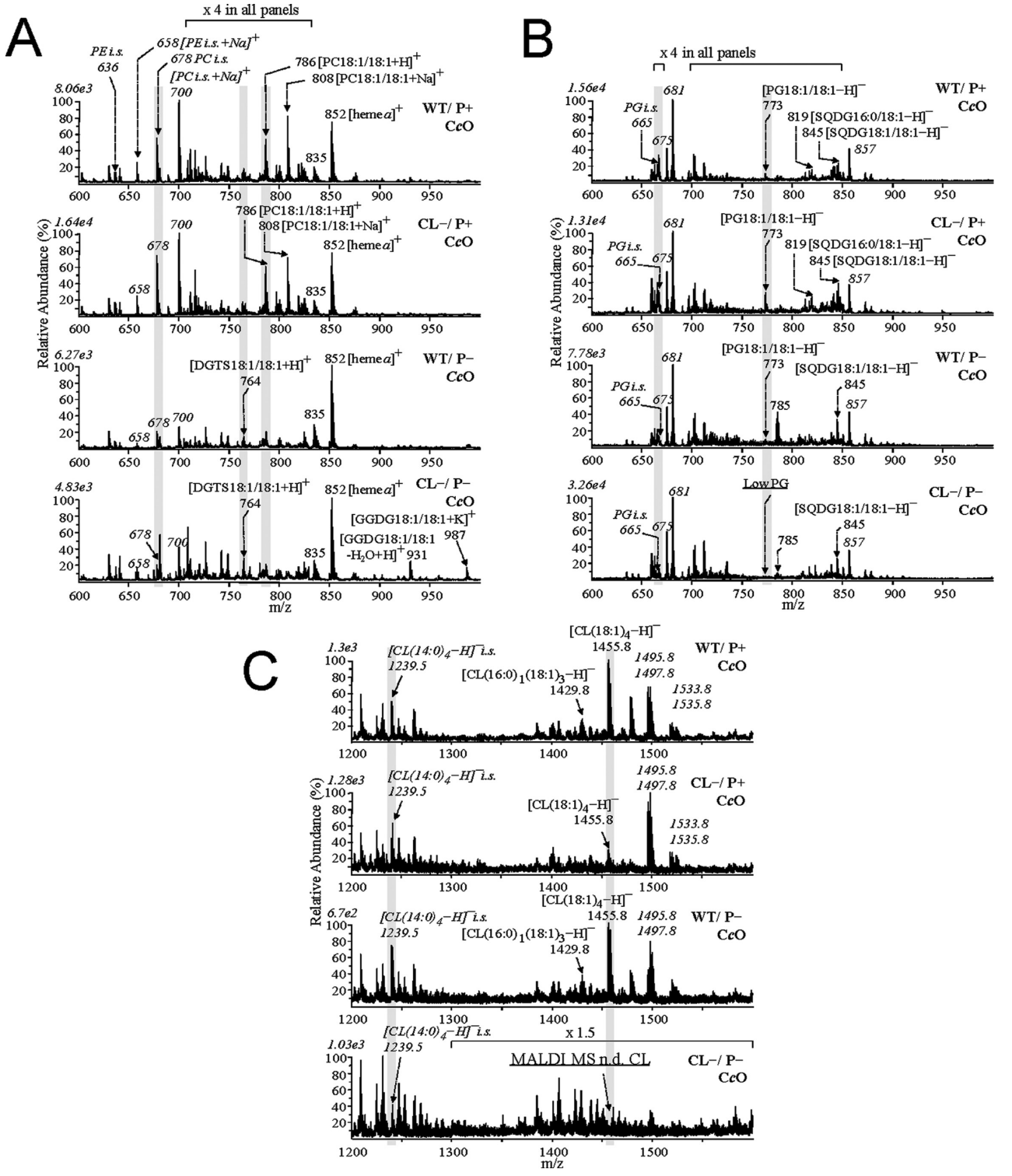

Figure 5. Direct MALDI MS analysis of lipids in the unextracted C*c*O purified from *R. sphaeroides* strains WT/P+, CL−/P+, WT/P−, and CL−/P−. Phospholipid internal standards (i.s.) allow for quantification of the lipid species. The strains and different growth conditions are described in Materials and Methods: (A) positive ion mode, (B) negative ion mode at m/z 600−1000, and (C) negative ion mode at m/z 1200−1600. As in Figure 4, m/z peaks of internal standards and lipids of particular interest are highlighted. In panel A under P− conditions, less PC (m/z 786 and 808) but more DGTS (m/z 764) is indicated. In panel B under P− conditions, loss of PG but retention of SQDG (m/z 845) is seen. In the bottom part of panel C, the P− conditions combined with the CL(−) mutant result in a major loss of CL (m/z 1455.8). These results are summarized in Table 2.

consistent with the results for the membrane determined by ESI (Tables 1 and 2).

The results from both the positive and the negative ion mode MALDI MS obtained for WT and CL− C*c*O produced under

dx.doi.org/10.1021/bi1017039 |*Biochemistry* 2011, 50, 3891–3902

Table 3. Possible Functional Interchangeability between Different Types of Lipids in Membranes and C*c*O from *R. sphaeroides* in Vivo

Head group charge	Non-PL	Phospholipids (PL)
Negative	QL	***Cardiolipin***
	SQDG	Phosphatidylglycerol
Zwitterionic: fixed	DGTS	Phosphatidylcholine
Zwitterionic: mobile	OL	Phosphatidylethanolamine
Neutral	GGDG	

P+ and P− growth conditions show clearly that in WT/P− C*c*O, the P-limited growth causes nearly complete depletion of PC and ~50% depletion of PG but maintains 70% of the level of CL (all percentages are relative to the levels in WT/P+ C*c*O). Concomitantly, increased levels of the non-phospholipids DGTS and SQDG are seen, similar to the membrane lipid composition changes characterized by ESI. These results demonstrate that when only P− growth is applied, the WT strain persistently synthesizes and incorporates cardiolipin in C*c*O and cell membranes with a much stronger preference over other phospholipids. However, in the P-limited growth combined with the CL− mutation, CL−/P− C*c*O is depleted of CL to below detectable levels and has a lower level of PG, increased levels of the non-phospholipid SQDG, and an obvious increase in the level of DGTS (m/z 764). These results show that CL−/P− C*c*O can maintain its native activity and enzyme properties through a mechanism other than selective enrichment of CL in the isolated enzyme. With major depletion of CL, PG, and PC, increases in the levels of the non-phospholipids DGTS, SQDG, and QL allow C*c*O to remain fully functional. With an abundant supply of phosphate, C*c*O has a preferential specificity for the CL lipid, but when CL cannot be synthesized efficiently, such a preference for CL can be substituted by a preference for PG. When both PG and CL are unavailable, the requirement for CL appears to be successfully replaced by negatively charged non-phospholipids such as SQDG and QL.

CONCLUSIONS

Phosphate-limited growth conditions caused significant selective changes in the lipid profiles of both the *Rhodobacter* membrane and purified cytochrome *c* oxidase. The bacteria under P− growth conditions display different priorities for making various types of lipids. The first priority is cardiolipin (70% maintained in P−), followed by PG (50% maintained), and the lowest priorities are PE and PC. These latter lipids appear to be successfully substituted by the non-phospholipids DGTS and OL, which contain a similar zwitterionic charge center. Levels of QL and SQDG were found to increase by 2−5-fold during P− growth, suggesting their functional substitution for phospholipids. The fact that purified WT/P− C*c*O maintains >70% of the CL level found in WT/P+ C*c*O indicates a significant preference of the bacteria for making CL rather than other phospholipids when phosphate-limited, suggesting that the structural features of CL are more important for the membrane and for C*c*O than PC or PE (even though six PEs are identified in the *Rs*C*c*O crystal structure[22]). The notable absence of CL containing $(18:2)_4$ in the bacterial system, which is the predominant (and more readily oxidized) form found in mammals,[23,24] may explain the difference in the absolute requirement for this unusual lipid species in diverse organisms.

Phosphate-limited growth combined with the *cls* mutation produced major changes in the lipid profile and a "cleaner" CL− depleted strain, in which the CL levels are reduced to <1% in the membrane and the purified enzyme, as revealed by both ESI and MALDI. Nevertheless, the resultant purified *R. sphaeroides* C*c*O was remarkably insensitive to the drastically modified lipid content, with regard to subunit composition, spectral properties, enzyme activity, protein expression level, and stability during purification.

These findings indicate that the entire structure of CL is not essential for the active form of bacterial C*c*O. The requirement for CL can be fulfilled by PG when available, because of its high degree of structural similarity with respect to negative charge and hydrogen bonding capacity. Further, the requirement for CL and/or PG can also be satisfied by non-phospholipids such as SQDG, and potentially QL, suggesting that the phosphate group can be replaced by negatively charged sulfite and carboxylic acid groups capable of ionic and hydrogen bond interactions. These observations extend the previous scheme of functional interchangeability between phospholipids to include non-phospholipids (Table 3).

In vivo manipulation of the lipid content of C*c*O by combined metabolic and genetic interventions, coupled with direct MS analysis of the membrane, the purified enzyme, and enzyme crystals, provides a powerful tool for further investigating the structural arrangement and dynamic roles of lipids in C*c*O.

ASSOCIATED CONTENT

Supporting Information. Structures of the lipid types of interest. This material is available free of charge via the Internet at http://pubs.acs.org.

AUTHOR INFORMATION

Corresponding Author

*Department of Biochemistry and Molecular Biology, Michigan State University, East Lansing, MI 48824. Phone: (517) 353-3512. Fax: (517) 353-9334. E-mail: fergus20@msu.edu.

Funding Sources

The work was supported by National Institutes of Health Grants R01 GM26916 (S.F.-M.) and the Michigan State University Center of Excellence for the Structural Analysis of Membrane Proteins (C.B., G.E.R., and S.F.-M.).

ABBREVIATIONS

C*c*O, cytochrome *c* oxidase; *cls*, cardiolipin synthase gene; CL, cardiolipin; PG, phosphatidylglycerol; PE, phosphatidylethanolamine; PC, phosphatidylcholine; OL, ornithine lipid; QL, glutamine lipid; SQDG, sulfoquinovosyldiacylglyceride; CL(+), cardiolipin-proficient strain; CL(−), cardiolipin-deficient strain; MALDI, matrix-assisted laser desorption ionization; nESI, nanoelectrospray ionization; MS, mass spectrometry; MS/MS, tandem mass spectrometry; MS^n, multistage tandem mass spectrometry; CID

MS/MS, collision-induced dissociation MS/MS; vMALDI, vacuum MALDI; MALDI-LIT, MALDI-linear ion trap; 2,5-DHB, 2,5-hydroxybenzoic acid; SDS−PAGE, sodium dodecyl sulfate−polyacrylamide gel electrophoresis; WT, wild type.

REFERENCES

(1) Benning, C., Huang, Z.-H., and Gage, D. A. (1995)Accumulation of a novel glycolipid and a betaine lipid in cells of *Rhodobacter sphaeroides* grown under phosphate limitation. *Arch. Biochem. Biophys. 317*, 103–111.

(2) Benning, C., Beatty, J. T., Prince, R. C., and Somerville, C. R. (1993)The sulfolipid sulfoquinovosyldiacylglycerol is not required for photosynthetic electron transport in *Rhodobacter sphaeroides* but enhances growth under phosphate limitation. *Proc. Natl. Acad. Sci. U.S.A. 90*, 1561–1565.

(3) Lopez-Lara, I. M., Gao, J.-L., Soto, M. J., Solares-Perez, A., Weissenmayer, B., Sohlenkamp, C., Verroios, G. P., Thomas-Oates, J., and Geiger, O. (2005)Phosphorus-free membrane lipids of *Sinorhizobium meliloti* are not required for the symbiosis with alfalfa but contribute to increased cell yields under phosphorus-limiting conditions of growth. *Mol. Plant-Microbe Interact. 18*, 973–982.

(4) Geiger, O., Rohrs, V., Weissenmayer, B., Finan, T. M., and Thomas-Oates, J. E. (1999)The regulator gene phoB mediates phosphate stress-controlled synthesis of the membrane lipid diacylglyceryl-N,N,N-trimethylhomoserine in *Rhizobium* (*Sinorhizobium*) *meliloti*. *Mol. Microbiol. 32*, 63–73.

(5) Benning, C., and Somerville, C. R. (1992)Isolation and genetic complementation of a sulfolipid-deficient mutant of *Rhodobacter sphaeroides*. *J. Bacteriol. 174*, 2352–2360.

(6) Arondel, V., Benning, C., and Somerville, C. R. (1993)Isolation and functional expression in *Escherichia coli* of a gene encoding phosphatidylethanolamine methyltransferase (EC 2.1.1.17) from *Rhodobacter sphaeroides*. *J. Biol. Chem. 268*, 16002–16008.

(7) Benning, C. (1998)Biosynthesis and function of the sulfolipid sulfoquinovosyl diacylglycerol. *Annu. Rev. Plant Physiol. Plant Mol. Biol. 49*, 53–75.

(8) Tamot, B. (2006) Construction and characterization of a cardiolipin-deficient mutant in *Rhodobacter sphaeroides*. M.S. Thesis, Department of Biochemistry and Molecular Biology, Michigan State University, East Lansing, MI.

(9) Chang, S.-C., Heacock, P. N., Mileykovskaya, E., Voelker, D. R., and Dowhan, W. (1998)Isolation and characterization of the gene (CLS1) encoding cardiolipin synthase in *Saccharomyces cerevisiae*. *J. Biol. Chem. 273*, 14933–14941.

(10) Xie, J., Bogdanov, M., Heacock, P., and Dowhan, W. (2006) Phosphatidylethanolamine and monoglucosyldiacylglycerol are interchangeable in supporting topogenesis and function of the polytopic membrane protein lactose permease. *J. Biol. Chem. 281*, 19172–19178.

(11) Sistrom, W. R. (1960)A requirement for sodium in the growth of *Rhodopseudomonas spheroides*. *J. Gen. Microbiol. 22*, 778–785.

(12) Sistrom, W. R. (1962)The kinetics of the synthesis of photopigments in *Rhodopseudomonas spheroides*. *J. Gen. Microbiol. 28*, 607–616.

(13) Zhen, Y., Qian, J., Follmann, K., Hayward, T., Nilsson, T., Dahn, M., Hilmi, Y., Hamer, A. G., Hosler, J. P., and Ferguson-Miller, S. (1998)Overexpression and purification of cytochrome c oxidase from *Rhodobacter sphaeroides*. *Protein Expression Purif. 13*, 326–336.

(14) Qin, L., Hiser, C., Mulichak, A., Garavito, R. M., and Ferguson-Miller, S. (2006)Identification of conserved lipid/detergent-binding sites in a high-resolution structure of the membrane protein cytochrome c oxidase. *Proc. Natl. Acad. Sci. U.S.A. 103*, 16117–16122.

(15) Hiser, C., Mills, D. A., Schall, M., and Ferguson-Miller, S. (2001)C-Terminal truncation and histidine-tagging of cytochrome *c* oxidase subunit II reveals the native processing site, shows involvement of the C-terminus in cytochrome *c* binding, and improves the assay for proton pumping. *Biochemistry 40*, 1606–1615.

(16) Hosler, J. P., Fetter, J., Tecklenburg, M. M. J., Espe, M., Lerma, C., and Ferguson-Miller, S. (1992)Cytochrome *aa3* of *Rhodobacter sphaeroides* as a model for mitochondrial cytochrome *c*-oxidase. Purification, kinetics, proton pumping, and spectral analysis. *J. Biol. Chem. 267*, 24264–24272.

(17) Awasthi, Y. C., Chuang, T. F., Keenan, T. W., and Crane, F. L. (1971)Tightly bound cardiolipin in cytochrome oxidase. *Biochim. Biophys. Acta 226*, 42–52.

(18) Zhang, X., and Reid, G. E. (2006)Multistage tandem mass spectrometry of anionic phosphatidylcholine lipid adducts reveals novel dissociation pathways. *Int. J. Mass Spectrom. 252*, 242–255.

(19) Gage, D. A., Huang, Z. H., and Benning, C. (1992)Comparison of sulfoquinovosyl diacylglycerol from spinach and the purple bacterium *Rhodobacter sphaeroides* by fast atom bombardment tandem mass spectrometry. *Lipids 27*, 632–636.

(20) Zhang, X., Ferguson-Miller, S. M., and Reid, G. E. (2009)Characterization of ornithine and glutamine lipids extracted from cell membranes of *Rhodobacter sphaeroides*. *J. Am. Soc. Mass Spectrom. 20*, 198–212.

(21) Zhang, X. (2009) Investigating the Functional Roles of Lipids in Membrane Protein Cytochrome *c* Oxidase from *Rhodobacter sphaeroides* Using Mass Spectrometry and Lipid Profile Modification. Ph.D. Thesis, Department of Chemistry and Department of Biochemistry and Molecular Biology, Michigan State University, East Lansing, MI.

(22) Svensson-Ek, M., Abramson, J., Larsson, G., Tornroth, S., Brzezinski, P., and Iwata, S. (2002)The X-ray crystal structures of wild-type and EQ(I-286) mutant cytochrome *c* oxidases from *Rhodobacter sphaeroides*. *J. Mol. Biol. 321*, 329–339.

(23) Chicco, A. J., and Sparagna, G. C. (2007)Role of cardiolipin alterations in mitochondrial dysfunction and disease. *Am. J. Physiol. 292*, C33–C44.

(24) Xu, Y., Malhotra, A., Ren, M., and Schlame, M. (2006)The enzymatic function of tafazzin. *J. Biol. Chem. 281*, 39217–39224.